Biosensors and Bioelectronics ■ (■■■■) ■■■–■■■

Contents lists available at ScienceDirect

Biosensors and Bioelectronics

journal homepage: www.elsevier.com/locate/bios

Piezometric biosensors for anti-apoptotic protein survivin based on buried positive-potential barrier and immobilized monoclonal antibodies

Magdalena Stobiecka [a,*], Agata Chalupa [b], Beata Dworakowska [a]

[a] Department of Biophysics, Warsaw University of Life Sciences, SGGW, 02-776 Warsaw, Poland
[b] Institute of Nanoparticle Nanocarriers, 11010 Barczewo, Poland

ARTICLE INFO

Article history:
Received 6 September 2015
Received in revised form
9 October 2015
Accepted 12 October 2015

Keywords:
Piezoimmunosensor
Protein survivin
Monoclonal anti-survivin antibody
Quartz crystal microbalance
Immunosensor

ABSTRACT

The anti-apoptotic protein survivin (Sur) plays an important role in the regulation of cell division and inducing the chemotherapeutic drug resistance. The Sur protein and its mRNA have recently been studied as cancer biomarkers and potential targets for cancer therapy. In this work, we have focused on the design of immunosensors for the detection of Sur based on buried positive-potential barrier layer structure and anti-survivin antibody. The modification of solid Au_{QC} piezoelectrodes was monitored by recording the resonance frequency shift and electrochemical measurements during each step of the sensor preparation. Our results indicate that the immunosensor with covalently bound monoclonal anti-survivin antibody can detect Sur with the limit of detection, LOD = 1.7 nM (S/N = 3σ). The immunosensor applicability for the analysis of real samples was assessed by testing samples of cell lysate solutions obtained from human astrocytoma (glioblastoma) U-87MG cell line, with the experiments performed using the standard addition method. The good linearity of the calibration curves for PBS and lysate solutions at low Sur concentrations confirm the high specificity of the proposed biosensor and good discrimination against nonspecific interactions with lysate components. The calculations indicate that there is still room to increase the Sur capture capacity for Sur while miniaturizing the sensor. The important advantage of the sensor is that it can be reused by a simple regeneration procedure.

1. Introduction

Advanced treatment modalities have recently been developed for cancer therapy marking considerable achievements on the way to curing this disease. However, the key challenge to a successful cancer treatment is the early diagnosis of the disease (Hanash et al., 2011; Yang et al., 2014). To that end, the design of simple and widely available biosensors capable of recognizing low grade neoplasia has become one of the important fields in the battle against cancer. In this work, we report on the development of a new biosensor for the detection of a cancer biomarker, protein survivin, strongly expressed in virtually all cancer types. The proposed biosensor is based on the immunorecognition technology and offers piezometric and electrochemical transductions.

Survivin (Sur) is a member of the group of inhibitor-of-apoptosis proteins (IAP). It plays a crucial role in the regulation of cell division and cell cycle control (Altieri, 2001; Ambrosini et al., 1997; Mita et al., 2008; Olie et al., 2000). Sur is also responsible for cancer cells resistance to chemotherapeutic drugs (Du et al., 2015). Sur is intensely expressed in the fetal organs and in a variety of cancer tissues but its level is very low in the normal differentiated cells (Altieri, 2001, 2008; Mita et al., 2008; Sah et al., 2006). By binding to caspase-3 and caspase-7, Sur is able to inhibit apoptosis and stimulate cell proliferation (Rubio et al., 2012). Sur protein and Sur mRNA have recently been extensively investigated in view of their potential utilization as selective targets for cancer therapy (Altieri, 2001, 2003, 2008).

For the determination of Sur level, most effective are the indirect methods based on the detection of messenger RNA (mRNA) expressed in cells for the Sur translation. Various fluorescent labeled oligonucleotide probes complementary to Sur mRNA have been designed, including fluorescent molecular beacons (MBs) for both the fixed cells (Peng et al., 2005) and the cells in a solution (Yang et al., 2005), dual-FRET system (Wang et al., 2011), peptide-linked probes (Nitin et al., 2004), DNA strands immobilized on graphite nanoparticles (Piao et al., 2012), and others. A beacon probe immobilized on a PMMA nanoparticle carrier has also been developed (Adinolfi et al., 2015) and tested with dermal fibroblasts HDFa by spiking with Sur mRNA. Carpi et al. utilized a 14 nucleotide (nt)

* Corresponding author. Fax: +48 22 593 8619.
E-mail address: magdalena_stobiecka@sggw.pl (M. Stobiecka).
URL: http://www.stobiecka.net (M. Stobiecka).

http://dx.doi.org/10.1016/j.bios.2015.10.041
0956-5663/

antisense MB to study the Sur expression in melanoma cells (Carpi et al., 2014). The length of the recognition sequence in the probes discussed above has often been very short (as short as 12-nt) making the probes ineffective, as indicated by the tumor screening sensitivity ranging from 21.1% (Johnen et al. 2012) (low-grade tumors) to 61.3% (Xue et al., 2011) (high-grade tumors only). Hence, the assays for Sur mRNA, despite of excellent performance in many cases, require further improvements in specificity and sensitivity, especially for low grade cancer detection. This became apparent in urinary tests for bladder cancer (Johnen et al., 2012) where the traditional cytology is still in use since the MB tests do not provide sufficient sensitivity.

On the other hand, direct methods of quantitative Sur protein determination are mostly based on molecular biology techniques including immunohistochemical methods (Gianani et al., 2001), Western blot (WB) (Kappler et al., 2003), ELISA analysis (Dobrzycka et al., 2015; Kappler et al., 2003; Konopka et al., 2009), and RT-PCR (Fu et al., 2008). Although very sensitive, these methods are time consuming and require highly specialized personnel. Nevertheless, these methods are suitable for the analysis of blood plasma where the Sur levels are extremely low (3.7 pM for healthy subjects and 9.1 pM for prostate cancer patients (Khan et al., 2012); 2.7 pM for healthy subjects and 6.8 pM for ovarian cancer patients (Dobrzycka et al., 2015)). The mass spectrometry methods (Khan et al., 2011) are also very sensitive and can be used for blood analysis but the high equipment cost is precluding their widespread use, especially in small labs.

Since the concentration of Sur in cell lysates is much higher (in the nM range) and the lysate can be easily prepared, therefore, the use of simple and inexpensive biosensors able to detect Sur protein or Sur mRNA in lysates has become a rational alternative to more traditional approaches. However, until now, there are only few reports on the development of biosensors for the detection of Sur mRNA. These biosensors were built on principles of DNA hybridization with fluorescence (Li et al., 2013; Piao et al., 2012) or electrochemical signaling (Liu et al. 2012). Recently, Li et al. (2013) have employed microfluidic microchannel devices and immobilized there antibodies against prostate stem-cell antigen (PSCA). They were able to capture prostate cancer cells and determine the Sur mRNA level in single cells by transfecting them with a graphene oxide nanocarrier preloaded with a fluorescent molecular beacon for direct mRNA analysis. They estimated the survivin mRNA content in single captured prostate cancer cell as $(4.8 \pm 1.8) \times 10^6$ copies corresponding to a concentration of 4.3 μM Sur mRNA. Also, a graphene nanoparticle sensor with adsorbed molecular beacon has successfully been applied for *in situ* Sur mRNA detection in cancer cells (Piao et al. 2012). Liu et al. (2012) have designed an electrochemical sensor based on dually labeled stem-loop DNA structure attached to a gold electrode to monitor the survivin mRNA in human hepatoma cell line (SMMC-7721).

To our knowledge, there are no publications on biosensors for Sur protein based on positive potential barrier SAM and anti-survivin antibodies. Hence, our investigations have focused on the design of Sur piezoimmunosensors and testing their basic characteristics to assess their utility for early cancer screening.

In our previous work (Stobiecka, 2014; Stobiecka and Chalupa, 2015b; Stobiecka et al., 2015), we have demonstrated that proteins can be determined with high sensitivity when employed for gating the plasmon-enhanced resonance energy transfer (RET) occurring between a fluorescent dye and a citrate-capped gold nanoparticle (AuNP). The gated-RET assay shows ultra-high sensitivity to Sur (the limit of detection, LOD = 240 pM (Stobiecka and Chalupa, 2015b)) but offers limited selectivity. The new piezometric biosensor developed in this work is somewhat less sensitive but provides high specificity since it is based on monoclonal anti-Sur antibodies. In addition to that, a convenient electrochemical transduction can also be used with this immunosensor offering low cost, fast response, and scalability useful for sensor miniaturization.

2. Materials and methods

2.1. Chemicals

Monoclonal antibody to survivin (Ab_{Sur}) and human survivin full length protein (Apoptosis Inhibitor Protein 4, AIP4), were purchased from Abcam (Cambridge, UK). Survivin (Sur) was purified by chromatography and tested by western blotting (purity: > 90% using 15% SDS-PAGE). It was stored in a solution of 0.1 M NaCl, 20 mM Tris, pH 7.5 at −70 °C. Aminohexanethiol (AHT), bovine serum albumin (BSA) and other agents were purchased from Sigma-Aldrich and used as received. All chemicals used for investigations were of analytical grade purity. Aqueous solutions were prepared with freshly deionized water with 18.2 MΩ cm resistivity (Hydrolab, Wiślina, Poland). All concentrations of added reagents cited in this paper are final concentrations obtained after mixing.

2.2. Apparatus

The nanogravimetric measurements were performed using an Electrochemical Quartz Crystal Nanobalance, Model EQCN-940 (Elchema, USA), with a Data Logger and Experiment Control System, Model DAQ-716v, operating under Voltscan 5.0 data acquisition and processing software. The resonant frequency f_0 of the Au-piezoelectrodes with 5 mm diameter Au disk was 9.975 MHz. The interfacial mass changes were determined from the changes in oscillation frequency of the quartz crystal resonator according to the Sauerbrey relationship fulfilled for thin rigid films (Sauerbrey, 1959). For quartz crystal resonators with 10 MHz fundamental resonance frequency, the relationship between film mass change Δm and the measured fundamental frequency shift Δf is given by: $\Delta m = -0.8673\ \Delta f$, where Δm is in ng and Δf is in Hz (Hepel, 1999; Hepel and Stobiecka, 2007; Stobiecka et al., 2005). The absence of viscoelastic effects has been confirmed in our earlier works using the Quartz Crystal Immittance (QCI) method (Stobiecka et al., 2005).

2.3. Preparation of immunosensor

Modification of gold electrodes was based on the buried positive-potential barrier layer structure (Stobiecka and Hepel, 2011) with aminohexanethiol (AHT) self-assembled monolayer (SAM), as presented in Fig. 1. The AHT-SAM was formed on a fresh gold piezoelectrode by immersing the electrode in 0.22 mM AHT ethanolic solution for 1 h. After washing the Au_{QC}@AHT sensor with ethanol and 10 mM PBS buffer, pH = 7.4, the antibody molecules were immobilized on the sensor surface by covalent attachment via amide bonds. The carboxylic groups of the Fc region of the Ab were first activated with a 5 mM EDC. The piezoelectrodes were incubated in solutions of different concentrations of monoclonal anti-Sur antibody (Ab_{Sur} solution + EDC + PBS buffer) for 60 min. Then, a BSA solution (0.01%) was applied for 60 min to block nonspecific binding sites. Finally, the biosensor was rinsed with PBS buffer pH 7.4 and kept in PBS buffer until use.

The stability of sensors was assessed by measuring the resonance frequency f_o.

The immunosensor regeneration procedure involved washing the sensors with an aqueous solution of glycine, pH 3.04, and rinsing with PBS buffer. It was developed basing on the method of Wasowicz et al. (2008).

Please cite this article as: Stobiecka, M., et al., Biosensors and Bioelectronics (2015), http://dx.doi.org/10.1016/j.bios.2015.10.041

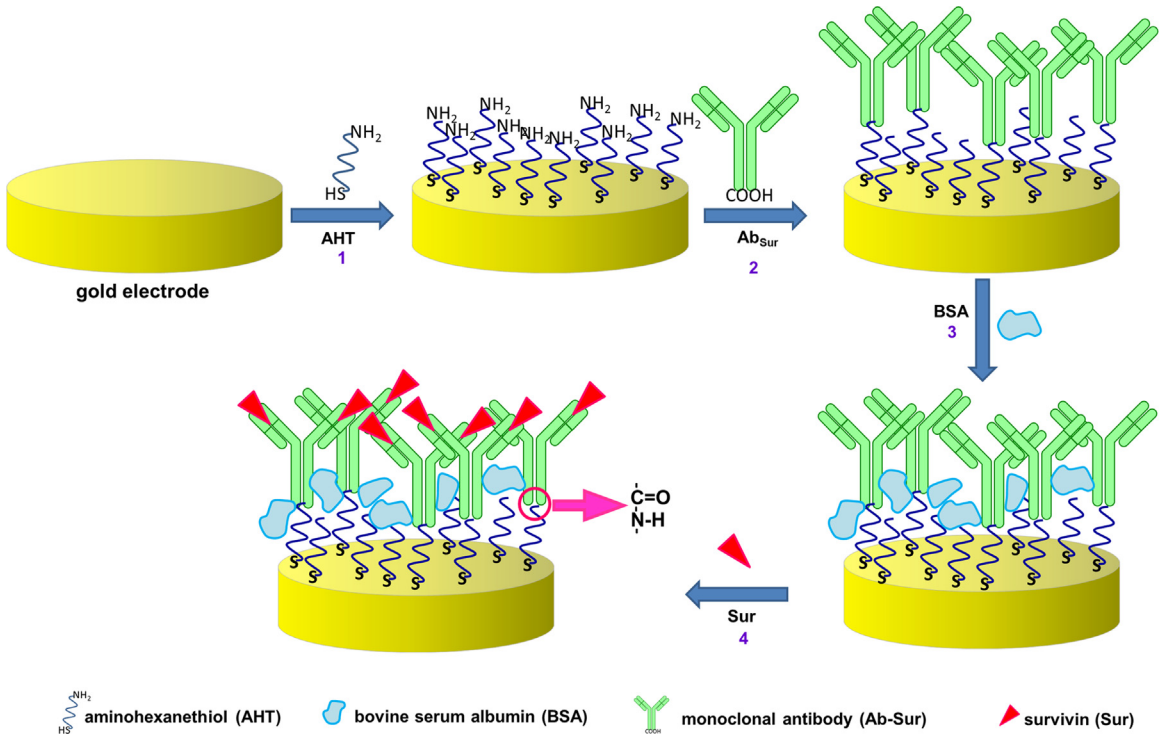

Fig. 1. Schematic illustration of the construction of immunosensors.

2.4. Data analysis

Linear or non-linear fitting of functions to the experimental data was performed using the Simplex algorithm embedded in the Origin graphing software (OriginLab, Northampton, MA, USA). Measurements were performed in triplicate unless otherwise stated. The reproducibility of the designed biosensors performance was strictly controlled. Sensors were constructed layer-by-layer with monitoring the resonance frequency of the piezoresonator substrates and CV characteristics. Sensor for which these monitoring functions deviated more than 10% were rejected. Since the recovery tests of the sensor quality, performed with cell lysate have shown that the recovery is monotonically dependent on analyte concentration, this dependence has been presented in Supplementary Material (Fig. S1).

3. Results and discussion

3.1. Nanogravimetric monitoring of the layer-by-layer biosensor construction

The modification of solid Au_{QC} piezoelectrodes was monitored by recording the resonance frequency shift during each step of the sensor preparation, as illustrated in Fig. 2. The frequency shift transients observed correspond to the film mass changes and confirm binding of molecules to the gold substrate or sensory film, according to the Sauerbrey equation relating the measured resonant frequency shift Δf to the film mass change Δm (Hepel, 1999; Hepel and Stobiecka, 2007; Sauerbrey, 1959):

$$\Delta f = -\frac{2\Delta m n f_0^2}{A\sqrt{\mu_q \rho_q}} \quad (1)$$

where f_0 is the series resonance frequency (fundamental mode) of an unperturbed QC resonator oscillation, n is the overtone number, A is the gold electrode (piezoactive) surface area, μ_q is the shear modulus of quartz ($\mu_q = 2.947 \times 10^{11}$ g cm^{-1} s^{-2}), and ρ_q is the quartz density ($\rho_q = 2.648$ g cm^{-3}).

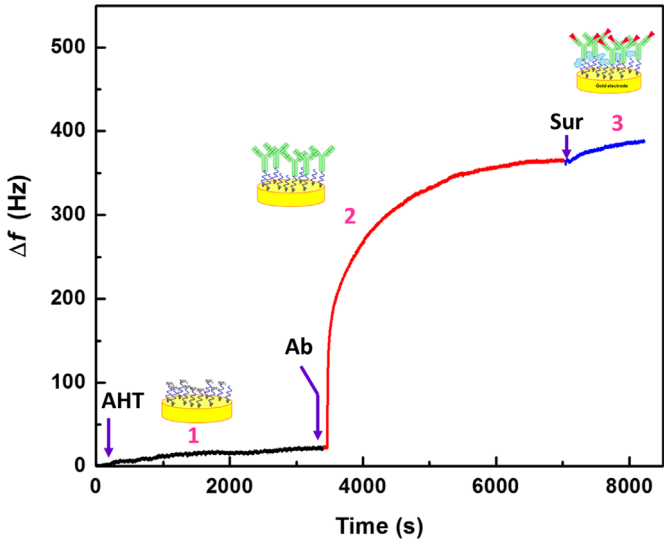

Fig. 2. Frequency shift transients for a piezosensor observed during: (1) AHT self-assembled monolayer adsorption on a Au piezoelectrode after injection of a AHT solution (0.22 mM, final concentration), followed by (2) covalent attachment of an EDC-activated anti-survivin monoclonal antibody (Ab_{Sur}) after injection of a Ab_{Sur} solution (3.23 μg/mL, final concentration), and (3) survivin (Sur) binding to a Au_{QC}@AHT/Ab_{Sur} after injection of a Sur solution (15.2 nM, final concentration). Arrows indicate the injections of AHT, Ab_{Sur} and Sur.

A typical frequency shift transient observed during the AHT-SAM formation on a gold piezoelectrode is presented in Fig. 2, curve (1). The total mass change for the adsorption of a monolayer of AHT is $\Delta m = 19.2$ ng ($\Delta f = 22.2$ Hz), after 3405 s. It corresponds to a surface coverage $\gamma_{AHT} = 6.64 \times 10^{-10}$ mol/cm^2 and monolayer mass $m_{mono,AHT} = 75.4$ ng/cm^2. This value agrees well with data reported by Imabayashi et al. (Imabayashi et al., 1997) for a close-packed monolayer of adsorbed alkanethiols obtained from the

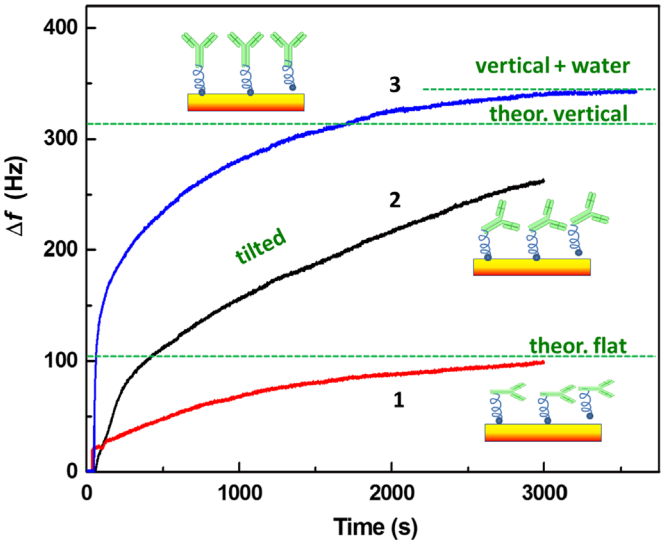

Fig. 3. Resonance frequency-shift transients observed during the formation of monolayer films of a monoclonal anti-survivin antibody (Ab_{Sur}) in PBS buffer pH 7.4 with Ab_{Sur} concentrations, c_{Ab} [μg/mL]: (1) 0.81, (2) 2.42, and (3) 3.23.

area of the reductive desorption peak. This confirms that a single monolayer of AHT is formed.

In the next step of the preparation of immunosensors, the monoclonal anti-survivin antibody was immobilized on a Au_{QC} @AHT sensor surface. The immobilization of an antibody is a crucial step due to the necessity of obtaining a correct Ab orientation to achieve a full access of the antigen to the Fab regions of the Ab. The density of Ab_{Sur} was optimized by checking the different concentrations of antibody on the surface of piezoelectrodes (Fig. 3). A typical nanogravimetric mass transient recorded after the injection of a monoclonal Ab_{Sur} aliquot is presented in Fig. 2, curve (2). The antibody, activated with a 5 mM solution of EDC, was immobilized covalently by amide bond formation between carboxylic $-COO^-$ groups on the surface of an Fc fragment of an antibody and the amine $-NH_3^+$ groups on the SAM on the surface of a piezoelectrode. For the concentration of antibody solution, $C_{Ab}=0.81$ μg/mL, the total mass change on the surface of the piezoelectrode was $\Delta m=84.8$ ng after 2990 s (Fig. 3, curve 1), with monolayer mass $m_{mono,Ab}=332.7$ ng/cm^2. For 2.42 μg/mL solution of Ab_{Sur} (Fig. 3, curve 2), $\Delta m=226.7$ ng and $m_{mono,Ab}=888.7$ ng/cm^2 were obtained. The highest concentration of Ab_{Sur} solution 3.23 μg/mL resulted in mass change $\Delta m=295.16$ ng and monolayer mass $m_{mono,Ab}=1157.5$ ng/cm^2 (Fig. 3, curve 3).

The theoretical total mass changes of a monolayer of antibody adsorbed on a QC surface based on dimensions of an antibody molecule (Fab arms: 6.5×3.5 nm, Fc stem: 5×3.5 nm, according to Brynda (2006)) have been estimated for vertical, side-on and flat orientations of Ab_{Sur} as follows: $\Delta m_{vert}=271.7$ ng, $\Delta m_{side}=168.20$ ng, $\Delta m_{flat}=90.6$ ng, respectively. The corresponding maximum theoretical monolayer mass for these orientations are: $m_{mono,vert}=1065.5$ ng/cm^2, $m_{mono,side}=659.6$ ng/cm^2 and $m_{mono,flat}=355.2$ ng/cm^2, and surface coverages $\gamma_{Ab,vert}=7.30$ pmol/cm^2, $\gamma_{Ab,side}=4.52$ pmol/cm^2, and $\gamma_{Ab,flat}=2.43$ pmol/cm^2, respectively. Hence, for the three concentrations of Ab_{Sur} in solution, three different orientations of antibodies attached to the AHT-SAM via amide bonds, can be envisioned: (a) for the lowest concentration (0.81 μg/mL), the anti-survivin antibody is in a horizontal orientation; (b) for higher concentration (2.42 μg/mL), Ab_{Sur} is likely to be tilted or in a side-on orientation with incorporation of solvent in film (the mass-percent of water in the Ab_{Sur} film is 26%); (c) for the highest concentration of Ab_{Sur} (3.23 μg/mL), a full monolayer of Ab_{Sur} in vertical orientation, with 8% of water in the film, has been found, consistent with the theoretical estimation of the Ab_{Sur} dimensions. Therefore, in subsequent experiments, the Ab_{Sur} concentration of 3.23 μg/mL was used for construction of biosensors to utilize the highest Sur capture capacity offered by the full monolayer of Ab_{Sur} in vertical orientation.

The mass change due to the binding of Sur on a Au_{QC}/AHT/Ab_{Sur},BSA-piezoelectrode is presented in Fig. 2, curve (3). For the concentration of survivin, $c_{Sur}=15.2$ nM, the total mass change on the surface of the piezoelectrode was $\Delta m=20.49$ ng after 1195 s (80.35 ng/cm^2), corresponding to 2.43 pmol/cm^2 (1.47×10^{12} molecules/cm^2). This surface concentration is lower than that calculated from the maximum possible concentration of capture sites on a full monolayer of Ab_{Sur} which is $\gamma_{Sur,max}=2\gamma_{Ab,mono,vert}=14.6$ pmol/cm^2. This means that ca. 17% of Ab capture centers are occupied by Sur analyte in this experiment. On the other hand, it follows from the crystallographic dimensions of Sur molecule ($5.47\times4.36\times5.63$ nm^3 (Chantalat et al. 2000)) that the Sur monolayer surface coverages for horizontal, side-on, and vertical orientations are: 5.39, 6.76, 6.96 pmol/cm^2, respectively. Therefore, the surface excess of the captured Sur corresponds to fractional coverage θ for horizontal orientation: $\theta=2.43/5.39=0.45$. These numbers indicate that the captured Sur molecules fill about half of a monolayer space while oriented horizontally. Hence, more Sur molecules can still be captured on the sensor surface in that orientation and possibly even more in tilted or vertical orientation. These calculations indicate that there is still room to increase the Sur capture capacity while miniaturizing the sensor. The miniaturization provides attractive features, including low consumption of expensive biochemical reagents, small sample requirement, and increase of mass transport due to the microdroplet effect (Yola et al., 2014; Zhang et al., 2013; Zhang et al., 2015). Further improvements of film capacity toward Sur analyte would need to rely on a 3D-structured sensing layer, as shown recently with Si-nanopilar coated biosensors (Rahman et al., 2015).

Note that in thin films, the hydration can be accounted for by calculating the mass of solution with the thickness of the deposited film. Then, the theoretical mass of the compounds forming the film assuming geometrical dimensions of molecules based on other measurements or electronic structure, can be calculated. Finally, the film mass determined experimentally (which consists of the organic compounds plus the solution remaining in the film), enables the estimation of the solution content in the film. While these are only estimates, the exact measurements of water content in films, which can be performed by measurements of neutron scattering, may be impractical due the requirements of neutron beams and sophisticated instrumentation. For the purpose of a sensor design, the estimates made are usually sufficient to draw important conclusions concerning the film structure. The experimental measurements confirm that considerable differences in the film mass are observed as the concentration of ligands in solution increases which is consistent with commonly observed change in the immobilized molecules' orientation from horizontal to vertical, proceeding with some changes in the degree of film hydration. While the trend of the changing tilt of immobilized molecules with increasing concentration of these molecules in the solution is generally known, it can be corroborated by the IR-RAS measurements. However, the main purpose of the measurements performed in this work was to control the immobilization of active biomolecules and maintain the film thickness within a single monolayer regime. The piezometric measurements together with the redox-probe electrochemical testing have enabled a precise control of the layer-by-layer sensory film synthesis. While the IR-RAS measurements can confirm the tilt, they are usually not suitable for a quantitative determination of the surface excess which is in the primary focus of the sensor design work.

Please cite this article as: Stobiecka, M., et al., Biosensors and Bioelectronics (2015), http://dx.doi.org/10.1016/j.bios.2015.10.041

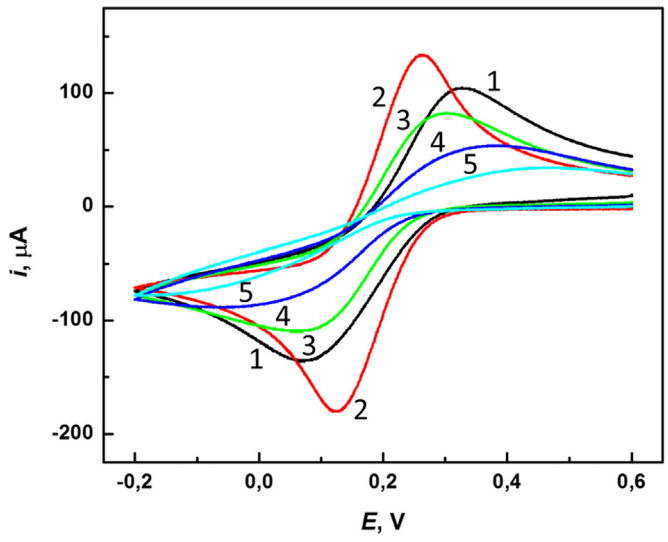

Fig. 4. Cyclic voltammograms for a 3.33 mM $K_3Fe(CN)_6$ probe in 66 mM phosphate buffer solution recorded after subsequent steps of the immunosensor construction: (1) bare gold piezoelectrode and (2–5) gold piezoelectrode after immobilization of successive layers of: (2) 6-amino-1-hexanethiol, (3) monoclonal anti-Sur antibody, (4) bovine serum albumin, (5) survivin; $v=100$ mV/s; electrolyte: 3.33 mM $K_3Fe(CN)_6$+66 mM PBS.

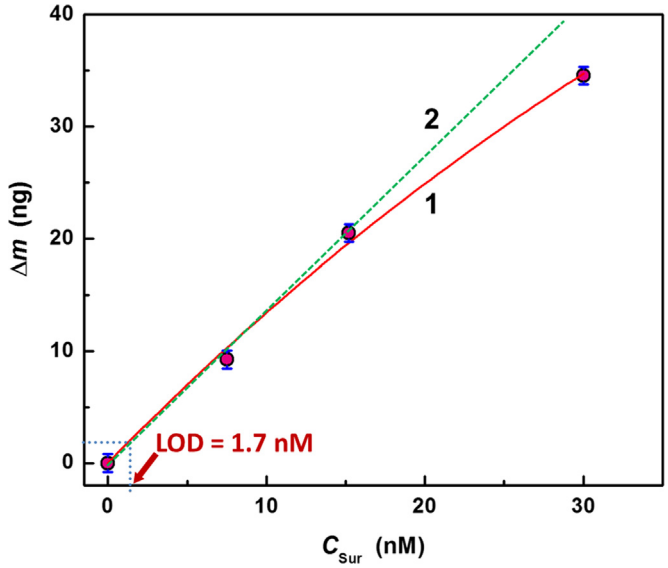

Fig. 5. Calibration plot of the apparent mass change Δm as a function of Sur concentration c_{Sur}, for a Au_{QC}/AHT/Ab_{Sur},BSA biosensor in 10 mM PBS, with surface regeneration in glycine solution, pH 3, after each test: (1) Langmuirian fitting function ($n=3$, $\sigma=0.799$, $R^2=0.997$), (2) linear fit at lower concentrations.

3.2. Electrochemical redox-probe testing of sensor functionalization

In support of the nanogravimetric monitoring of the sensor construction, the electrochemical measurements utilizing the electroactive redox probe, $Fe(CN)_6^{3-}$, were performed. Fig. 4 presents cyclic voltammetry characteristics obtained after consecutive steps of the gold piezoelectrode modification in a 3.33 mM $K_3Fe(CN)_6$+66 mM PBS solution. For bare gold electrode (Fig. 3, curve 1), a pair of well-defined quasi-reversible redox peaks was observed ($E_{red}=0.069$ V, $E_{ox}=0.330$ V).

The deposition of a self-assembled AHT monolayer caused an increase in current intensity and a decrease in the peak separation for the redox marker to $\Delta E_p=141$ mV (Fig. 4, curve 2). Since the dissociation constants for AHT are $pK_1=8.19$ (-NH_3^+) and $pK_2=10.75$ (-SH), the predominant form of AHT at pH=7.4 is a

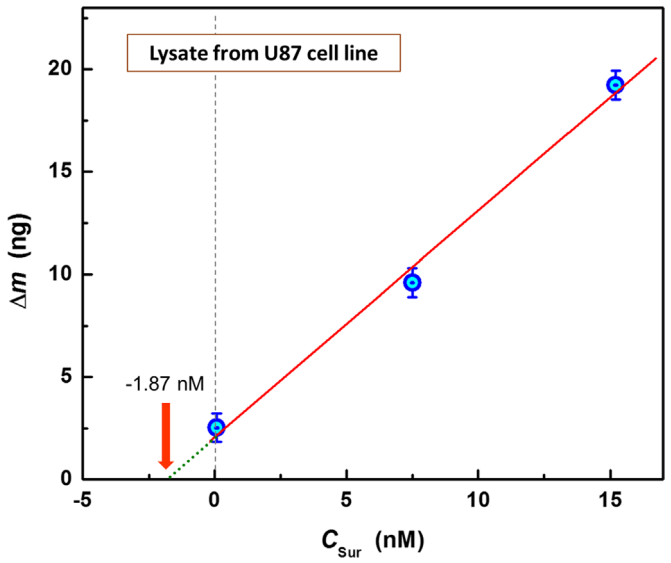

Fig. 6. Test of Sur determination by the standard addition method in a lysate solution obtained from the human astrocytoma (glioblastoma) U-87 MG cell line, using a Au_{QC}/AHT/Ab_{Sur},BSA biosensor, with surface regeneration in glycine solution of pH 3 after each test; 1:5 dilution of lysate in 10 mM PBS.

cation with a single positive charge on the amine group (-NH_3^+). The protonation of amine groups and the formation of a positively charged barrier film promotes the electron transfer between the redox molecules and the electrode surface.

The immobilization of Ab_{Sur} molecules which are negatively charged at pH 7.4 (Fig. 4, curve 3) caused a decrease in current intensity and an increase in the peak separation for the redox couple $Fe(CN)_6^{3-}/Fe(CN)_6^{4-}$ to $\Delta E_p=245$ mV due to the diminished surface accessibility and steric hindrance.

The addition of 0.01% BSA solution (Fig. 4, curve 4) caused more blocking effect and increase in the peak separation to $\Delta E_p=316$ mV.

As seen in Fig. 4, curve 5, the addition of Sur with negative net charge (the isoelectric point of survivin $pI=5.66$) to the immunosensor leads to considerable decrease of the system reversibility and results in a decrease of the electroactive marker response. The experimental results are consistent with the expected behavior associated with the repulsive nature of interactions between negative redox marker and negatively charged molecules of an antibody and proteins: BSA and survivin.

3.3. Detection of survivin

The dependence of the apparent mass change on survivin concentration for a Au_{QC}/AHT/Ab_{Sur},BSA piezoimmunosensor is presented in Fig. 5.

The nonlinear fitting of a Langmuirian function of the form:

$$\Delta m = m_{max}\frac{K_a c_{Sur}}{(1+K_a c_{Sur})} \quad (2)$$

to the experimental data by least-squares regression using a Simplex algorithm provides the following parameter values: $m_{max}=166.5$ ng, $K_a=0.00878$ nM^{-1}, $n=3$, $\sigma=0.799$, $R^2=0.997$, for c_{Sur} in [nM] and Δm in [ng]. The limit of detection for Sur is then calculated from the Eq. (2) for $\Delta m=3\sigma$, as follows:

$$LOD = c_{Sur,LOD} = \frac{3\sigma}{K_a(m_{max}-3\sigma)} \quad (3)$$

The low value, LOD=1.7 nM, was obtained.

Table 1
Comparison of survivin detection characteristics for the proposed immunosensor and assays for survivin analysis in cell lysates.

System	Method	Detection Limit[a]	References
AuNP@Cit/Sur, FITC	gated RET[b]	0.240 ± 0.007 nM (synthetic solutions)	Stobiecka and Chalupa, 2015b
DuoSet IC-ELISA; R&D Systems	ELISA[c]	2.8 to 32.6 ng per mg protein in tumor cell lysates (17 to 199 nM)[a]	Kappler et al., 2003
Rabbit anti-human survivin antibody and horseradish peroxidase-labeled goat anti-rabbit IgG	WB[d]	N.S. detected Sur in 11 out of 14 tumor cell lysates in high Sur content (score 2 or 3) tumors	Kappler et al., 2003
Anti-survivin antibody and peroxidase -labeled goat anti-rabbit antibody	IHA[e]	N.S.; detected Sur: 20/20 in normal colonic mucosa, 20/20 in hyperplastic polyps, 20/20 adenomatous polyps, 20/20 in colonic adenocarcinomas	Gianani et al., 2001
Human Total Survivin TiterZyme Enzyme Immunometric Assay (EIA) kit	ELISA	5.8 ± 2.3 to 24.3 ± 2.9 ng survivin/mg proteins in cancer cells lysates (35 ± 14 to 148 ± 18 nM)[a]	Konopka et al., 2009
Exosomes	WB	N.S.	Khan et al., 2011
Au_{QC}/AHT/Ab_{Sur},BSA	EQCM biosensor	1.87 ± 0.7 nM in lysate solution; 1.7 ± 0.8 nM in 10 mM PBS	This work

[a] Detection limit: N.S.–not specified; numbers in parenthesis–nM concentrations calculated for comparison, assuming typical protein content of 100 mg/mL in lysates;
[b] gated RET–gated resonance energy transfer;
[c] ELISA–enzyme-linked immunosorbent assay;
[d] WB–western blot;
[e] IHA–Immunohistochemical analysis.

3.4. Sensor testing in cell lysate and the recovery tests

The applicability of the proposed immunosensor for the analysis of real samples was tested using sample solutions based on cell lysate. A 1:5 dilution of a lysate solution obtained from the human astrocytoma (glioblastoma) U-87 MG cell line in PBS was used in the piezometric measurements with a Au_{QC}/AHT/Ab_{Sur},BSA biosensor. The experiments were carried out using the standard addition method with the original diluted lysate sample and two samples spiked with 7.5 and 15 nM Sur (final concentrations). The linear least-square fitting performed for the obtained experimental data is presented in Fig. 6 on the plot of mass change Δm *vs.* c_{Sur} with extrapolation of the line to the intercept with abscissa. The negative intercept represents the intrinsic Sur concentration in lysate solution and is equal to $-c_{Sur,lys}$. The obtained value of $c_{Sur,lys}$ = 1.87 nM. The parameters of the line ($\Delta m = ac_{Sur} + b$) are as follows: y-intercept $b = 2.064 \pm 0.843$ ng, slope $a = 1.105 \pm 0.086$ ng/nM, coefficient of determination $R^2 = 0.996$, $n = 3$, rsdev = 1.32%. This level of Sur in cell lysate is consistent with values recently determined for a lysate of cancer cells (5.8 to 24.3 ng/mg of proteins (Konopka et al., 2009); assuming the total protein concentration in lysate of 2 mg/mL, it leads to the Sur level of ca. 1 to 3 nM).

The low standard deviation and good linearity of the calibration indicate that the proposed biosensor discriminates well against nonspecific interactions with the lysate components. Note, however, that the slopes of the calibration lines in Fig. 5 for PBS buffer and in Fig. 6 for lysate of U87 cell line differ slightly (1.3485 and 1.1050 ng/nM, respectively). Because of the small slope difference, the experimental recovery tests show changes of the recovery with analyte concentration. For instance, for Sur concentrations in the range from 2 to 15 nM, the recovery changes from 92.0% to 83.1%. The dependence of the recovery on Sur concentration is presented in the Supplementary Material (Fig. S1).

A comparison of the methods applied for Sur determination in cell lysates is presented in Table 1. It is seen that the sensitivity of the proposed biosensor fits well to the range of Sur concentrations encountered in cell lysates from various tumors.

4. Conclusions

We have demonstrated that piezometric and voltammetric immunosensors based on positive potential barrier SAM of AHT and a monoclonal anti-survivin antibody Ab_{Sur} can be designed and used for the detection of survivin with a low limit of detection, LOD = 1.7 nM. It follows from the performed optimization experiments that at least 3.2 μg/mL of Ab_{Sur} is necessary to form a full monolayer of vertically oriented Ab_{Sur} and covalently bonded to the AHT SAM. Tests conducted with human astrocytoma (glioblastoma) U-87MG cell line lysate indicate that there are good linear responses of the sensor to Sur additions at low concentrations. This means that the sensor discriminates well against the nonspecific interactions with lysate components and provides high measurement specificity for Sur determination. Further enhancements of the proposed immunosensor performance are possible by miniaturization and taking advantage of the mass transport acceleration by microdroplet technology. We are also engaged in investigations of Sur release by cancer cells via exosomes (Stobiecka and Chalupa, 2015a) which may offer a new way of reducing metastasis and chemoresistance (Khan et al., 2011).

Acknowledgments

This research was supported by funding provided by the Grant Iuventus Plus, No. IP2012058072 awarded by the MSHE.

Appendix A. Supplementary material

Supplementary data associated with this article can be found in the online version at http://dx.doi.org/10.1016/j.bios.2015.10.041.

References

Adinolfi, B., Pellegrino, M., Baldini, F., 2015. Biomed. Pharmacother. 69, 228–232.
Altieri, D.C., 2001. Trends Mol. Med. 7, 542–547.
Altieri, D.C., 2003. Nat. Rev. Cancer 3 56-54.

Altieri, D.C., 2008. Nat. Rev. Cancer 8, 61–70.
Ambrosini, G., Adida, C., Altieri, D.C., 1997. Nat. Med. 3, 917–921.
Brynda, E., 2006. Methods for attachment of antibodies onto optical biosensors. Opt. Chem. Sens., 387–401.
Carpi, S., Fogli, S., Giannetti, A., Adinolfi, B., Tombelli, S., Pozzo, E.D., Vanni, A., Martinotti, E., Martini, C., Breschi, M.C., Pellegrino, M., Nieri, P., Baldini, F., 2014. PLoS One 9 (12), e114588.
Chantalat, L., Skoufias, D., Kleman, J., Jung, B., Dideberg, O., Margolis, R., 2000. Mol. Cell 6, 183–189.
Dobrzycka, B., Mackowiak-Matejczyk, B., Terlikowska, K.M., Kulesza-Bronczyk, B., Kinalski, M., Terlikowski, S.J., 2015. Tumor Biol. 36, 4157–4165.
Du, J., Li, B., Fang, Y., Liu, Y., Wang, Y., Li, J., Zhou, W., Wang, X., 2015. BMC Cancer 15, 536.
Fu, S., Cai, J., Tu, Z., Wang, Y., Deng, L., Liang, Z., Lin, Z., Gong, X., 2008. Chin.-Ger. J. Clin. Oncol. 7, P523–P526.
Gianani, R., Jarboe, E., Orlicky, D., Frost, M., Bobak, J., Lehner, R., Shroyer, K.R., 2001. Hum. Pathol. 32, 119–125.
Hanash, S.M., Baik, C.S., Kallioniemi, O., 2011. Nat. Rev. Clin. Oncol. 8, 142–150.
Hepel, M., 1999. Electrode–solution interface studied with electrochemical quartz crystal nanobalance. In: Wieckowski, A. (Ed.), Interfacial Electrochemistry. Theory, Experiment, and Applications. M. Dekker, New York, pp. 599–631.
Hepel, M., Stobiecka, M., 2007. Bioelectrochem 70, 155–164.
Imabayashi, S.I., Hobara, D., Kakiuchi, T., 1997. Langmuir 13 (17), 4502–4504.
Johnen, G., Gawrych, K., Bontrup, H., Pesch, B., Taeger, D., Banek, S., Kluckert, M., Wellhaußer, H., Eberle, F., Nasterlack, M., Leng, G., Stenzl, A., Bruning, T., 2012. PLOS One 7 (4), e35363 35361-35310.
Kappler, M., Kotzsch, M., Bartel, F., Fussel, S., Lautenschlager, C., Schmidt, U., Wurl, P., Bache, M., Schmidt, H., Taubert, H., Meye, A., 2003. Clin. Cancer Res. 9, 1098–1104.
Khan, S., Jutzy, J.M.S., Aspe, J.R., McGregor, D.W., Neidigh, J.W., Wall, N.R., 2011. Apoptosis 16 (1), 1–12.
Khan, S., Jutzy, J.M.S., Valenzuela, M.M.A., Turay, D., Aspe, J.R., Ashok, A., Mirshahidi, S., Mercola, D., Lilly, M.B., Wall, N.R., 2012. PLoS ONE 7 (10), e46737.
Konopka, K., Spain, C., Yen, A., Overlid, N., Gebremedhin, S., Duzgunes, N., 2009. Cell. Mol. Biol. Lett. 14, 70–89.
Li, X.-L., Shan, S., Xiong, M., Xia, X.-H., Xu, J.-j, Chen, H.-Y., 2013. Lab Chip 13, 3868–3875.
Liu, J., Zhou, H., Xu, J.J., Chen, H.Y., 2012. Analyst 137, 3940–3945.
Mita, A.C., Mita, M.M., Nawrocki, S.T., Giles, F.J., 2008. Clin. Cancer Res. 14, 5000–5005.
Nitin, N., Santangelo, P.J., Kim, G., Nie, S., Bao, G., 2004. Nucleic Acids Res. 32, e58.
Olie, R.A., Simoes-Wust, A.P., Baumann, B., Leech, S.H., Fabbro, D., Stahel, R.A., Zangemeister-Wittke, U., 2000. Cancer Res. 60, 2805–2809.
Peng, X.H., Cao, Z.H., Xia, J.T., Carlson, G.W., Lewis, M.M., Wood, W.C., Yang, L., 2005. Cancer Res. 65, 1909–1917.
Piao, Y., Liu, F., Seo, T.S., 2012. ACS Appl. Mater. Interfaces 4, 6785–6789.
Rahman, M.M., Adalian, D., Scherer, A., 2015. J. Nanotechnol 2015, 467190.
Rubio, N., Garcia-Segura, L.M., Arevalo, M.A., 2012. J. Neurovirol 18 (5), 354–363.
Sah, N.K., Khan, Z., Khan, G.J., Bisen, P.S., 2006. Cancer Lett. 244, 164–171.
Sauerbrey, G., 1959. Z. Phys. 155, 206–222.
Stobiecka, M., 2014. Biosens. Bioelectron. 55, 379–385.
Stobiecka, M., Chalupa, A., 2015a. Chem. Pap. 69 (1), 62–76.
Stobiecka, M., Chalupa, A., 2015b. J. Phys. Chem. B 119 (41), 13227–13235. http://dx.doi.org/10.1021/acs.jpcb.5b07778.
Stobiecka, M., Chalupa, A., Dworakowska, B., 2015. MRS Proc 1720, 52–58.
Stobiecka, M., Hepel, M., 2011. Biosens. Bioelectron 26, 3524–3530.
Stobiecka, M., Hepel, M., Radecki, J., 2005. Electrochim. Acta 50, 4873–4887.
Wang, Z.Q., Zhao, J., Zeng, J., Wu, K.J., Chen, Yl, Wang, X.Y., Chang, L.S., He, D.L., 2011. Acta Pharmacol. Sinica 32, 1522–1528.
Wasowicz, M., Viswanathan, S., Dvornyk, A., Grzelak, K., Kłudkiewicz, B., Radecka, H., 2008. Biosens. Bioelectron 24, 284–289.
Xue, Y., An, R., Zhang, D., Zhao, J., Wang, X., Yang, L., He, D., 2011. Eur. J. Obstet. Gynecol. Reprod. Biol. 159, 204–208.
Yang, L., Cao, Z., Lin, Y., Wood, W.C., Staley, C.A., 2005. Cancer Biol. Therapy 4 (5), 561–570.
Yang, T.L., Lin, L., Lou, P.J., Chang, T.C., Young, T.H., 2014. PLoS One 9 (1), e86143.
Yola, M.L., Atar, N., Eren, T., 2014. Sens. Actuat. B - Chem 198, 70–76.
Zhang, H., Jia, Z., Lv, X., Zhou, J., Chen, L., Liu, R., Ma, J., 2013. Biosens. Bioelectron 44, 89–94.
Zhang, M., Huang, J., Cui, W., Pang, W., Zhang, H., Zhang, D., Duan, X., 2015. Biosens. Bioelectron. 74, 8–15.

Please cite this article as: Stobiecka, M., et al., Biosensors and Bioelectronics (2015), http://dx.doi.org/10.1016/j.bios.2015.10.041